Electronic Supplementary Material (ESI) for Nanoscale.

Supplementary information for "Proton irradiation of graphene: insights from atomistic modeling"

Tan Shi[a], Qing Peng[a], Zhitong Bai[b], Fei Gao[a] and Igor Jovanovic*[a]

[a] Department of Nuclear Engineering and Radiological Sciences, University of Michigan, Ann Arbor, Michigan 48109, USA
[b] Department of Mechanical Engineering, University of Michigan, Ann Arbor, Michigan 48109, USA
*E-mail: ijov@umich.edu

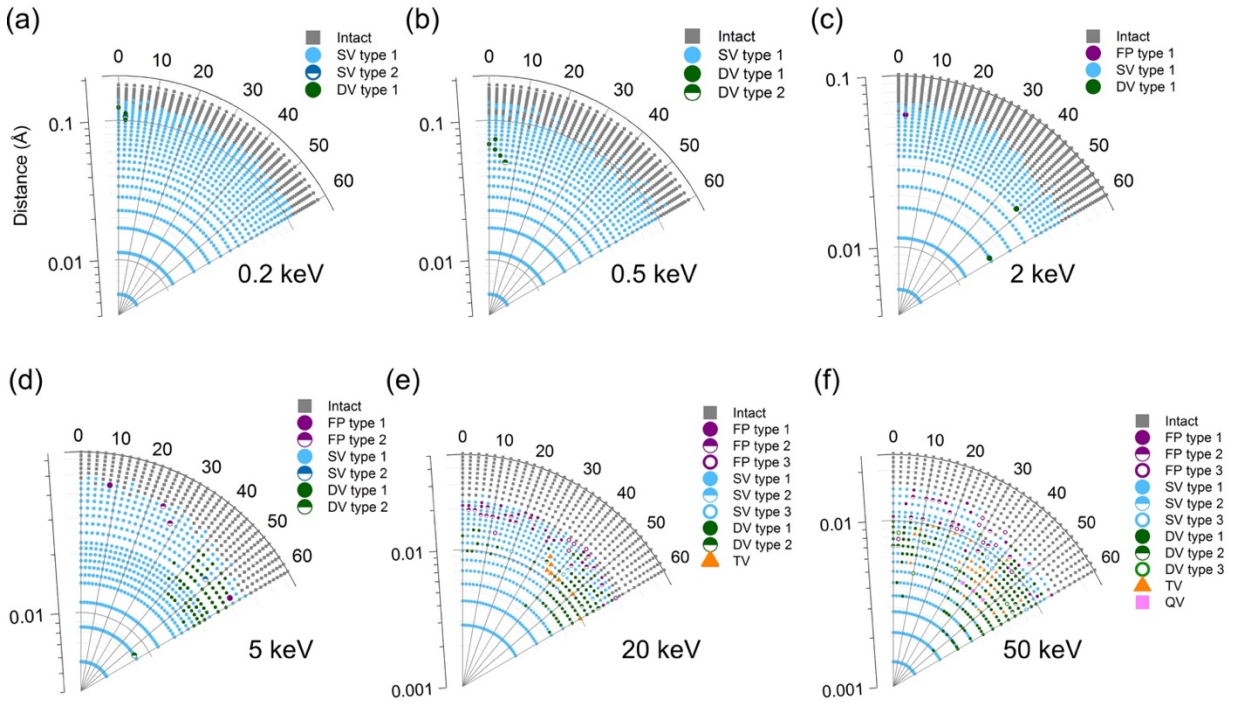

Figure S1. Defect types as a function of the impact position of the proton for an incident energy of **(a)** 0.2 keV, **(b)** 0.5 keV, **(c)** 2 keV, **(d)** 5 keV, **(e)** 20 keV and **(f)** 50 keV at normal incidence simulated with the LAMMPS code. The origin of the polar coordinate system is the position of the selected carbon PKA and the marker positions correspond to the proton impact positions. For defect configurations with no, one, two, three and four atoms being ejected out of the simulation system, they are labeled as Frenkel pair (FP, purple), single vacancy (SV, blue), double vacancies (DV, green), triple vacancies (TV, orange) and quad-vacancies (QV, pink) respectively.

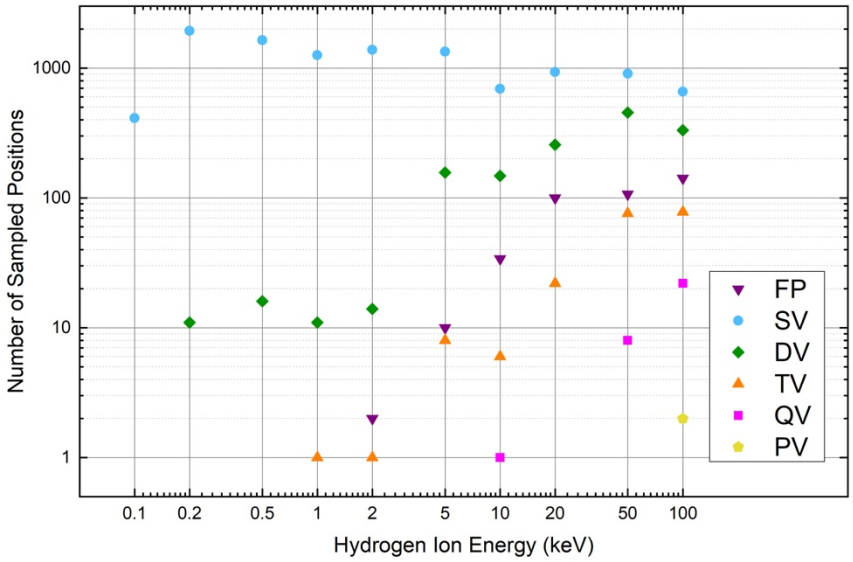

Figure S2. The number of sampled ion positions for different proton energies at a normal incidence angle simulated with the LAMMPS code. The defect generation probabilities presented in **Figure 4** of the manuscript were determined based on the number of sampled positions shown here.

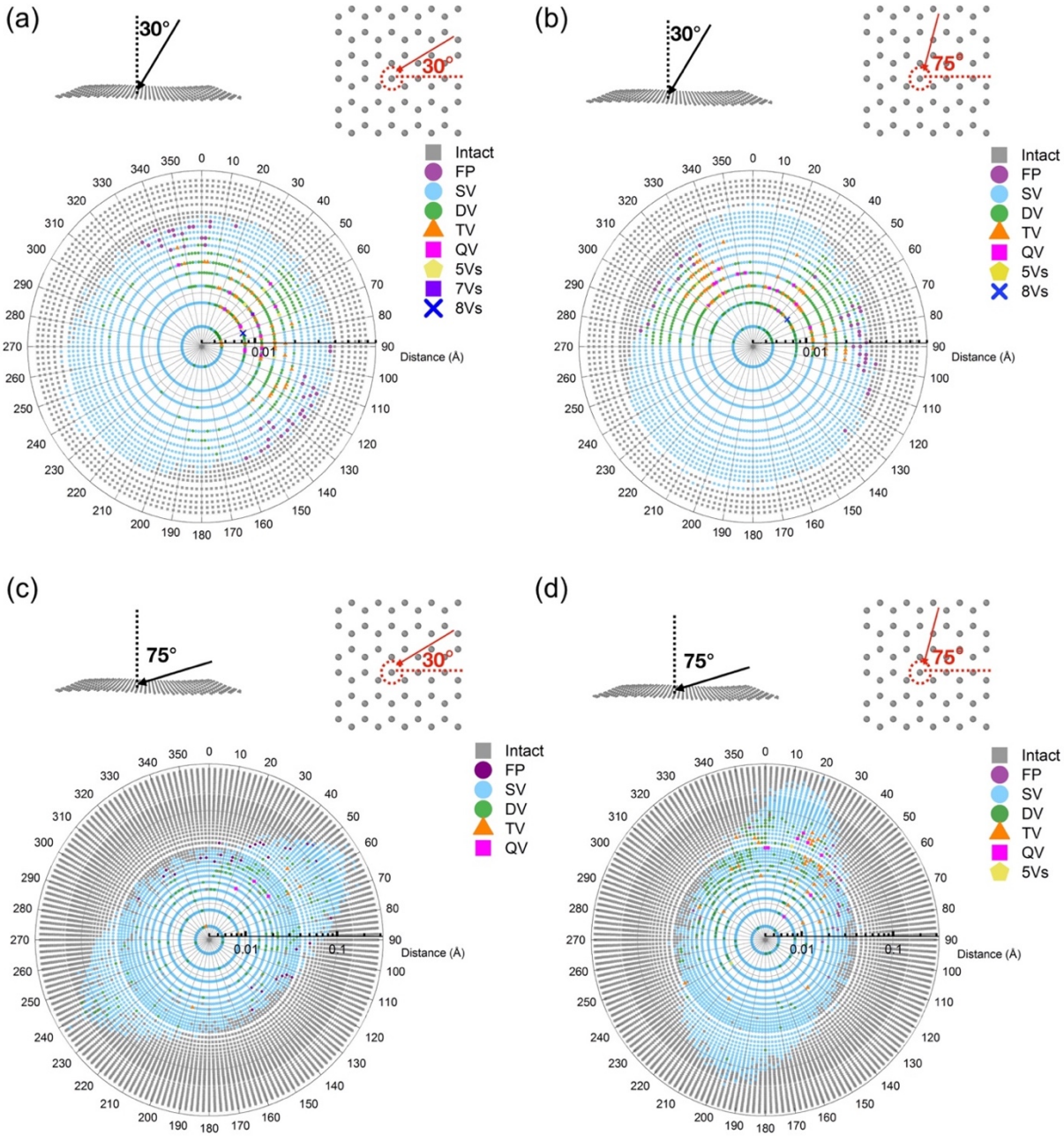

Figure S3. Defect types as a function of the impact position of the proton for an incident energy of 10 keV at different azimuthal incident angles. The study was performed at a polar angle 30° and 75°. At a polar angle of 30°, the results for an azimuthal angle of **(a)** 30° and **(b)** 75° are shown here. At a polar angle of 75°, the results for an azimuthal angle of **(c)** 30° and **(d)** 75° are shown here. The relationships between the incident angle, impact position and graphene structure lead to the differences shown in this figure.

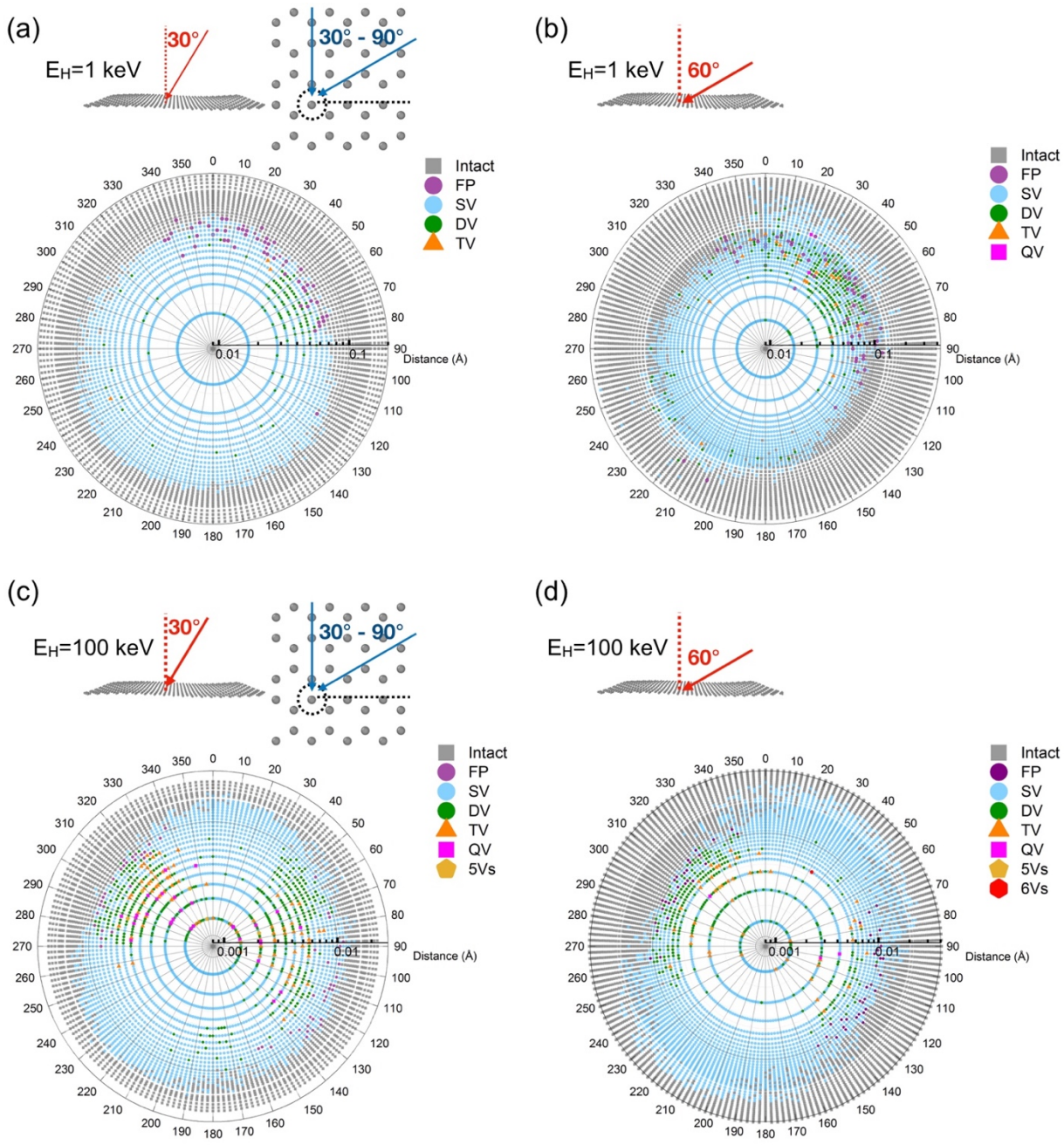

Figure S4. Defect types as a function of the impact position of the proton at different polar angles. At an incident energy of 1 keV, the results were shown for a polar angle of **(a)** 30° and **(b)** 60° respectively. At an incident energy of 100 keV, the results were shown for a polar angle of **(c)** 30° and **(d)** 60° respectively. The azimuthal angle was randomly sampled between 30° and 90° due to the crystal symmetry. The SV probability increases with the polar angle, as manifested by the elongated impact area along the proton direction. At 1 keV, a significant increase of the DV probability can be observed from (a) to (b). In comparison, there is only a moderate change at 100 keV, as shown from (c) to (d).

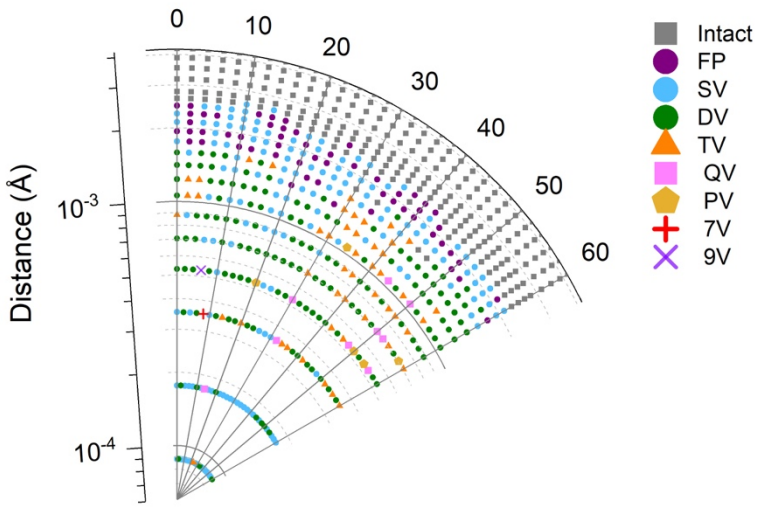

Figure S5. Defect types as a function of the impact position of the proton for an incident energy of 2 MeV at normal incidence simulated with the LAMMPS code. For defect configurations with no, one, two, three, four, five, seven and nine atoms being ejected out of the simulation system, they are labeled as FP (Frenkel pair), SV (single vacancy), DV (double vacancies), TV (triple vacancies), QV (quad-vacancies), PV (penta-vacancies), 7V and 9V, respectively.